2023 لسنة A10 العدد
No10A - Septembr 2023
المجلة العراقية للبحوث الانسانية والاجتماعية والعلمية
Iraqi Journal of Humanitarian, Social and Scientific Research
Print ISSN 2710-0952-Electronic ISSN 2790-1254

COVID-19 CT image detection using based-ANN deep learning method

Nibras A.Mohammed Ali[1], Firas A.Mohammed Ali[2]

[1]*Department Computer Science, College of Education for Women, University of Baghdad, Baghdad, Iraq*

[2]*Center for Strategic and International Studies, University of Baghdad, Baghdad, Iraq*

[*] Nebras.Ali@coeduw.uobaghdad.edu.iq , Firas.A.843@cis.uobaghdad.edu.iq

Abstract

In 2019, a novel coronavirus pneumonia (COVID-19) outbreak occurred, which substantially impacted the expansion of the global economy and the livelihoods of individuals. As a novel approach to image processing, a deep learning network has been developed and applied in clinical contexts to extract medical Information from CT images. However, due to the medical characteristics of COVID-19 CT scans, the lesions are widely dispersed and exhibit various local features. Consequently, using the current deep learning model for direct diagnosis is difficult. CT scans for COVID-19 medical features. We used an Artificial Neural Network, conventional classifiers, and deep learning to identify COVID-19. MRI images of various pneumonia sizes, locations, morphologies, and intensities were gathered to train the model. SVM classifiers and many activation algorithms were used to check our work. Python, TensorFlow, and Keras are used to execute our proposed solution. In our study, artificial neural networks (ANN) obtained an accuracy of 98.14 percent, which exceeds the current best-case scenario. Our ANN-based model will assist physicians in precisely identifying pneumonia in MRI scans, thereby expediting treatment.

Keywords: Coronavirus, CT Images, Artificial Neural Network, Artificial Neural Networks

الكشف عن صور الاشعة المقطعية لمرض كورونا باستخدام التعلم العميق عن طريق خوارزمية الشبكة العصبية الاصطناعية

نبراس محمد علي [1] ، فراس أحمد محمد علي [2]

1 قسم علوم الحاسوب ، كلية التربية للبنات ، جامعة بغداد ، بغداد ، العراق

2 مركز الدراسات الاستراتيجية والدولية ، جامعة بغداد ، بغداد ، العراق

خلاصة

في عام 2019 ، تفشى الالتهاب الرئوي الناجم عن فيروس كورونا الجديد ، مما أثر بشكل كبير على توسع الاقتصاد العالمي وسبل عيش الأفراد. كنهج جديد لمعالجة الصور ، تم تطوير شبكة التعلم العميق وتطبيقها

[*] Nebras.Ali@coeduw.uobaghdad.edu.iq
[*] Nebras.Ali@coeduw.uobaghdad.edu.iq

في السياقات السريرية لاستخراج المعلومات الطبية من صور التصوير المقطعي المحوسب. ومع ذلك ، نظرًا للخصائص الطبية لفحص كورونا المقطعي المحوسب ، فإن الآفات منتشرة على نطاق واسع وتظهر ميزات محلية مختلفة. وبالتالي ، فإن استخدام نموذج التعلم العميق الحالي للتشخيص المباشر أمر صعب. لفحص بالتصوير المقطعي المحوسب للميزات الطبية لمرض كورونا استخدمنا شبكة عصبية اصطناعية ومصنفات تقليدية وتعلم عميق للتعرف على الاصابة بفايروس كورونا تم جمع صور التصوير بالرنين المغناطيسي من مختلف أحجام الالتهاب الرئوي والمواقع والتشكيلات والشدة لتدريب النموذج. تم استخدام مصنفات خوارزمية آلة المتجهات الداعمة والعديد من خوارزميات التنشيط للتحقق من عملنا. يتم استخدام لغة بايثون و TensorFlow وKerasلتنفيذ الحل المقترح. في دراستنا ، حصلت الشبكات العصبية الاصطناعية على دقة بلغت 98.14 في المائة ، وهو ما يتجاوز أفضل سيناريو حالي. سيساعد نموذجنا المستند إلى لشبكات العصبية الاصطناعية الأطباء في تحديد الالتهاب الرئوي بدقة في فحوصات التصوير بالرنين المغناطيسي ، وبالتالي تسريع العلاج.

الكلمات المفتاحية: فيروس كورونا ، صور التصوير المقطعي المحوسب ، الشبكة العصبية الاصطناعية

1. Introduction

Medical imaging refers to a range of non-invasive techniques utilized to examine the internal structures of the human body [1]. Medical photos are used for diagnosis and treatment. Consequently, it significantly influences enhancing human health and therapeutic interventions. The efficacy of image processing at an advanced level is contingent upon the picture segmentation procedure, which constitutes a crucial and indispensable stage [2]. The focus of our investigation has been primarily directed toward the segmentation of MRI images, specifically those depicting cases of New Coronavirus Pneumonia. Facilitating the localization of pneumonia is a benefit afforded by the approach above to medical care. Medical image processing involves the use of three-dimensional images of the human body, which are typically acquired through computed tomography (CT) or magnetic resonance imaging (MRI) scanners. These pictures help with everything from studying disease to preparing for surgery. Medical image processing is used by radiologists, engineers, and doctors to learn more about a patient's or a group's unique structure. Using measurable features, statistical analysis, and computer models incorporating accurate anatomical geometries [3]. It is possibly better to understand the relationship between human anatomy and medical equipment. Pneumonia is a medical condition characterized by inflammation and accumulation of fluid or pus in the air sacs of one or both lungs.

2. Categorization of Pneumonia

There are four fundamental varieties of pneumonia, as depicted in Figure (1):

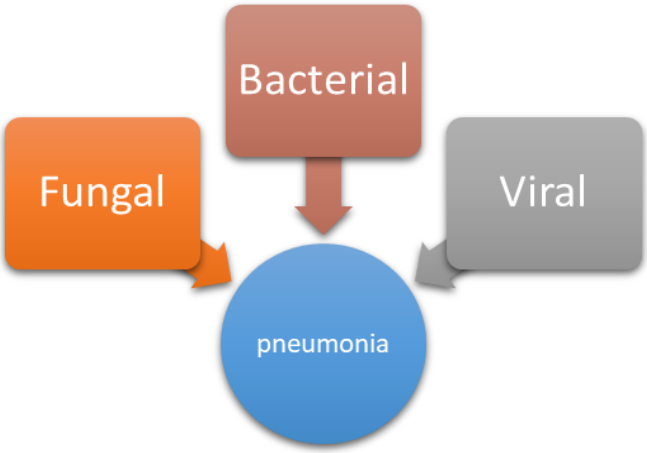

Fig1: Basic Types of Pneumonia.

2.1 Bacterial pneumonia

Streptococcus pneumonia is the predominant bacterium responsible for this condition. Pneumonia can potentially impact either the entirety of an individual's lung or a limited segment thereof. Although bacterial pneumonia may not pose an immediate threat, it can cause harm if it exerts pressure on vital structures such as blood vessels.

2.2 Fungal pneumonia

The inhalation of large quantities of fungi derived from soil or bird droppings can lead to pneumonia in susceptible individuals. Individuals with compromised immune systems, such as those diagnosed with Acquired Immunodeficiency Syndrome (AIDS), are commonly afflicted by a specific form of pneumocystis jirovecii pneumonia. (PCP).[4]

2.3 Mycoplasma pneumonia.

The inhalation of large quantities of fungi from soil or bird droppings can lead to pneumonia in susceptible individuals. Individuals with compromised immune systems, such as those diagnosed with Acquired Immunodeficiency Syndrome (AIDS), are commonly afflicted by a specific form of pneumocystis jirovecii pneumonia (PCP).

2.4 Viral pneumonia

This particular form of pneumonia, constituting approximately one-third of cases, is caused by various viruses, including the recently emerging coronavirus. (COVID-19). The initial onset of viral pneumonia may render individuals more vulnerable to the subsequent development of bacterial pneumonia. In its

developmental stage, the novel coronavirus induces acute pneumonia, and the manifestation of the disease may vary among individuals. Specific individuals may be infected with the pathogen, yet remain asymptomatic, whereas others may exhibit mild symptoms such as fever, fatigue, and coughing[4].

Conversely, some individuals may experience severe symptoms, including acute dyspnea and reduced oxygen saturation levels within the body. This statement lacks context and clarity. It is unclear what the user is referring to.

Further Information is needed to provide an academic rewrite. Enhancing the precision of previously proposed methodologies is imperative in the progression of medical imaging research. The paper suggests an ANN approach with 98.14% accuracy. Automating MRI image interpretation helps medical representatives speed up therapy[5].

3. Methods

The segmentation methods for pneumonia can be categorized into three distinct categories. The methodologies encompass manual, semi-automatic, and fully automatic approaches. The required level of user engagement can be determined based on its corresponding quantity [6].

3.1. Manual segmentation methods

The interpretation of MRI scans necessitates the expertise of a medical specialist who must integrate the depicted data with their acquired knowledge of anatomy and physiology through both academic instruction and practical experience. Pneumonia diagnosis requires a healthcare expert to examine multiple photos in succession. Manual separation is time-consuming and doctor-dependent, but results are highly variable [7]. This method is often used to perform fully automated and semi-automated methodologies.

3.2. Methods of semi-automatic segmentation

Academic literature indicates that user input is required for initialization, intervention or feedback response, and assessment [8]. Establishing a region of interest (ROI) that limits the anticipated pneumonia area facilitates initialization of the automated algorithm. Images can be preprocessed in various ways. Automated algorithms can be guided by input at launch and throughout the process. Furthermore, alterations are implemented consequently to this procedure. If the outcomes fail to meet the user's expectations, they may evaluate and iterate the process or make necessary modifications [9]. This methodology entailed the utilization of the algorithm across multiple applications. This technique involves training and classification methods within the context of pneumonia segmentation,

thereby transforming the segmentation task into a classification task. Many pneumonic MRI scan images from diverse cases are typically necessary to develop a machine-learning classification methodology to segment pneumonia. The outcome above is required for noise management and intensity bias correction. Under this methodology, the user initiates the process by selecting a subset of voxels associated with each tissue category from a single case. In this study, voxel-by-voxel classification of tissue categories in an image is performed using a support vector machine (SVM) technique. As features for training the SVM model, intensity values and spatial coordinates extracted from voxel subsets are used. The semi-automatic strategy for pneumonia segmentation not only requires less time compared to the manual approach but also yields effective outcomes. However, it is crucial to note that intra- and inter-rater user variability still exists with this method[10].

3.3. Absolute automated separation

The individual is under no compulsion to act in this fashion. Significant progress has been made in resolving the segmentation problem by integrating AI and contextual Information.

3.3.1. Challenges

Automated segmentation of pneumonia is a critical and complex task. The complexity of pneumonia MRI data derived from artificial databases or clinical scans is inherent. This has been noted in previous research [11]. MRI devices and acquisition methods can vary from scan to scan, resulting in intensity biases and other variances for each image segment. Differentiating PH subregions requires multiple modalities, which complicates the issue.

https://www.kaggle.com/code/madz2000/pneumonia-detection-using-cnn-92-6-accuracy

3.3.2 Pneumonia Dataset Description

From the dataset, train, test, and validation folders have been created. Within the dataset, each image category, namely Pneumonia and Normal, has its own subfolder. The dataset contains 4613 JPG X-Ray images classified as Pneumonia or Normal. The study selected anterior-posterior chest X-ray images from retrospective cohorts of twenty-to-sixty-year-olds at the Guangzhou Women and Medical Center. The individual received standard clinical care, which included periodic chest X-ray imaging. Before being excluded from the chest radiograph dataset, each image was subjected to an initial quality control evaluation. Before receiving authorization for AI system training, the diagnostic accuracy of the

photographs was evaluated by two skilled physicians. A third expert reviewed the evaluation set to guarantee the accuracy of the grading[12].

4. Proposed methodology

Artificial neural networks represent a systematic approach employed to analyze medical images. Artificial Neural Networks (ANNs) represent a specialized category of computational models for tasks such as image recognition and knowledge extraction from complex systems. Artificial neural networks (ANN) perform generative and descriptive tasks, utilizing deep learning as a powerful image-processing computational method. Machine vision, recommender systems, and language communication processes are commonly utilized in this context. Machine vision is capable of identifying images and videos. Recommender systems aid in suggesting relevant content. Language communication processes facilitate effective communication. (NLP). A neural network is a hardware- and software-based computational system that functions similarly to the biological neurons present in the human brain. There are three distinct layers in artificial neural networks: the input layer, the output layer, and one or more hidden layers. The nodes in the input layer must establish connections with the nodes in the hidden layer, while the nodes in the hidden layer establish connections with the nodes in the output layer. The input layer receives data from the network. The application of this particular image processing technique is not well-suited for implementation within an artificial neural network. This study presents an Artificial Neural Network (ANN) that utilizes a layered architecture designed to operate with minimal processing demands. The removal of restrictions and increased potency of image processing has resulted in a significantly more effective and easily trainable system for image and linguistic communication processes. Modifying the hidden layer has resulted in a significantly enhanced version of the artificial neural network model. The optimal outcomes for pneumonia detection are achieved by utilizing the fourteen phases incorporated in our layered artificial neural network model and including hidden layers[13]. The proposed methodology is illustrated in Figure 1, accompanied by a concise description.

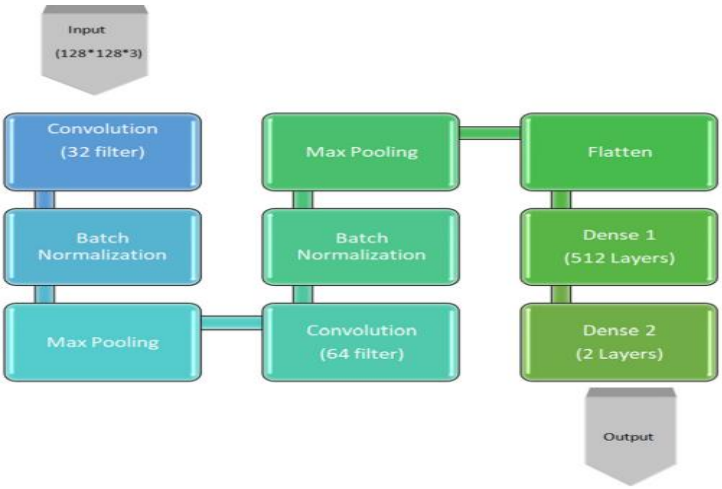

Fig. 2. Proposed methodology for pneumonia detection using layers of Artificial Neural Networks

$$Dice(P,T) = \frac{|P_1 \hat{} T_1|}{(|P_1| + |T_1|)/2}$$

The proposed method was to utilize a variety of photographic images as input, which were then transformed to conform to standard dimensions of 128 x 128 x 3. Using tri-channel tensors and 32 convolutional filters, each with a dimension of 2 by 2, our objective is to generate a complex convolutional kernel. The activation feature of ReLU is a characteristic that practitioners frequently utilize. The Rectified Linear Unit (ReLU) is a piecewise linear activation function that directly outputs the input if it is positive and returns zero if it is negative. Consequently, the bulk normalization technique proposed by Sergey Ioffe and his colleagues [14] was implemented. 2015 is the year in issue. Batch normalization, also known as the batch norm, normalizes the input to the layers by re-centering and re-scaling, resulting in enhanced stability and increased efficiency in neural networks. This strategy is described in reference [15]. This allowed for the rapid development of our algorithm. Please refer to Illustration 2. A two-dimensional filter is then applied to each channel of the feature map, followed by a summing of the features that fall within the filter's coverage region. The output dimensions for a feature map with dimensions after a pooling layer $n_h * n_w * n_c$ is

$$(n_h - f + 1)/s * (n_w - f + 1)/s * n_c$$

Where:

- ➔ n_h - height of feature map
- ➔ n_w - width of feature map
- ➔ n_c - no. of channels in the feature map
- ➔ f - size of filter

Hierarchically arranged convolutional and pooling layers constitute the conventional architecture of an Artificial Neural Network (ANN) model. Pooling layers is used to decrease the file size of feature maps. Consequently, fewer parameters are used to compute the network's duty. The pooling layer summarizes the features extracted from multiple feature maps generated by a convolutional layer. In lieu of precisely positioned features generated by the convolutional layer, summarized features are utilized to perform supplementary computations.

As a result, the model is more resistant to inconsistencies in the positioning of features within the input image. This study utilized a (2*2) Max pooling technique [16], in which the filter selects the maximal value from the feature map within its coverage range. Consequently, the output of the max-pooling layer would be a feature map containing the most significant features of the previous feature map. Referring to Figure 3, please. Following this step, 64 convolutional filters were utilized in conjunction with batch normalization and max-pooling techniques, followed by flattening. We proposed a neural network architecture with two layers of dense connectivity. The initial layer contains (512) hidden units, while the succeeding layer contains two additional hidden units. Given that the softmax activation function produces greater precision than other activation functions, we used it as the final layer's activation function. The loss function employed was "categorical cross-entropy," and the optimization algorithm was RMSProp, an extension of gradient descent and Adaptive.

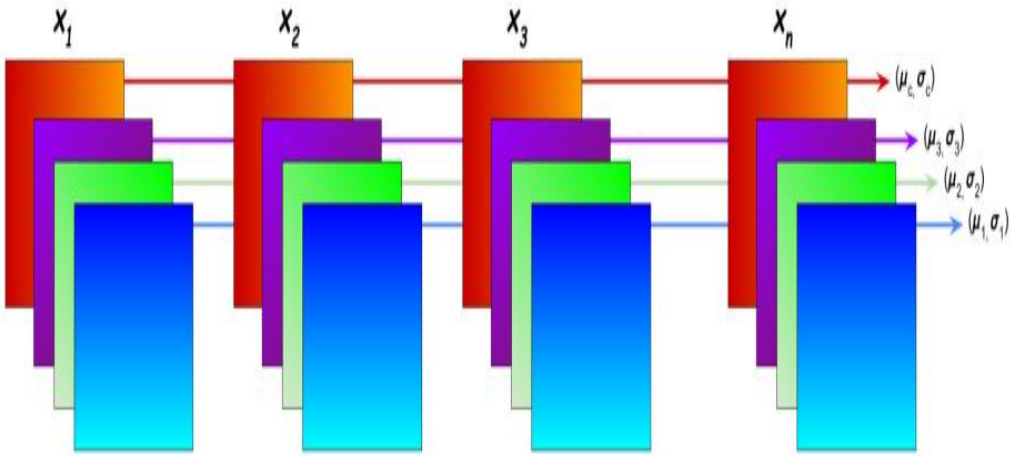

Fig. 3. Batch normalization.

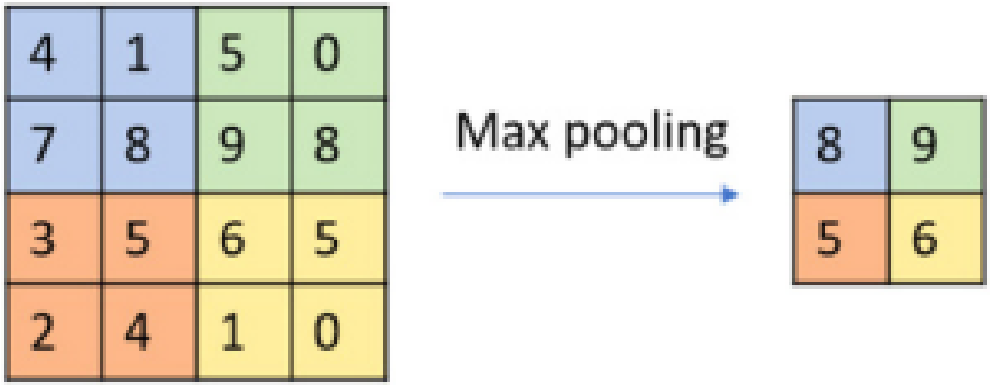

Fig. 4. (2*2) Maxpooling.

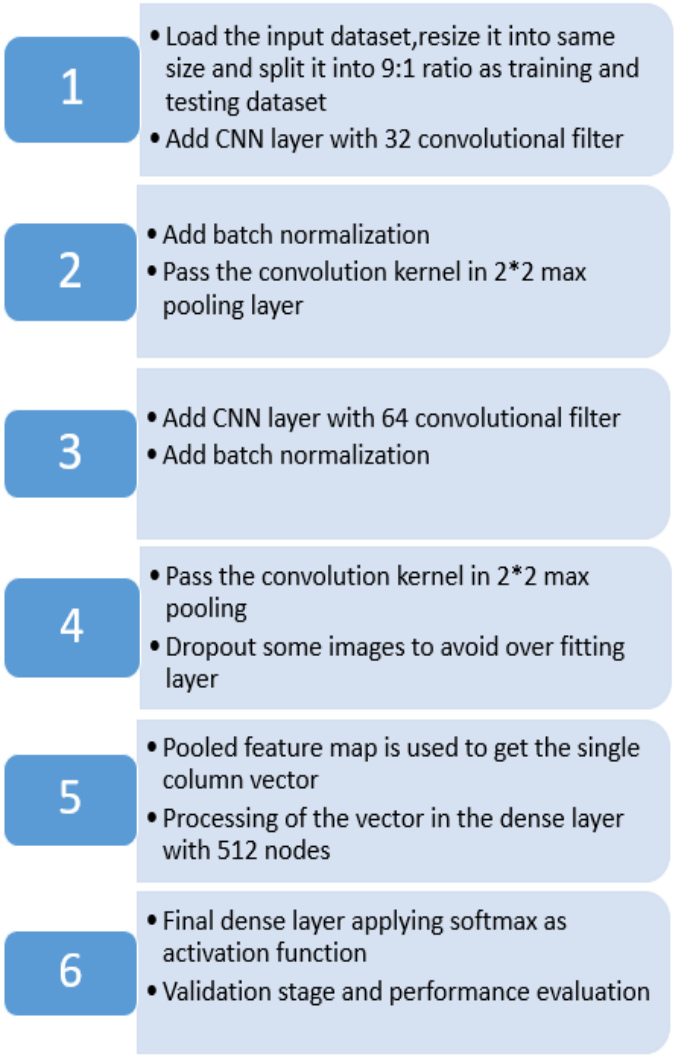

Fig. 5. The procedure for the suggested CNN model to work.

As an optimizer, gradient descent uses the Gradient Algorithm, which modifies the step size for each parameter based on a declining average of partial gradients. The steps involved in running the suggested Artificial Neural Network (ANN) model are shown in Figure 4. Table 1 below displays a comparison of various versions.

Table 1: Comparison of different models.

Final Layer Activation Method	Optimizer	Accuracy (%)	Testing Accuracy (%)	Evaluation of the Model (%)
SVM	N/A	12.17	17.33	22.33
Sigmoid	RMSProp	95.85	43.66	54.90
Softmax	AdaMax	96.3	64	77.89
Softmax	RMSProp	**98.14**	91.99	96.13

5. The Outcomes of Experiments

5.1. data set Information gathered in an experiment

The 2020 Chest X-Ray Pictures (Pneumonia) dataset was utilized in the experiment conducted for this research. A total of 4613 photographs were captured. The dataset comprises two distinct categories: class 1 pertains to photographs of pneumonia, and class 0 pertains to images of lungs that are deemed healthy. Figures 5 and 6 illustrate the datasets pertaining to healthy lungs and pneumonia, as obtained from the input photos.

5.2. Results and discussion

The results of our experimentation involving different artificial neural network models, activation functions, and optimizers have been presented in Tables 1 and 2. The AdaMax algorithm, an extension of the Adam Optimization algorithm for adaptive movement estimation, was the initial approach employed. The study yielded a 98.14% accuracy rate by implementing softmax in the final layer, with RMSProp as the optimizer. The model was trained on 4613 images and tested on 252 images, with a 9:1 splitting ratio. This can be viewed as a generalization of the Gradient Descent Optimization method. To mitigate the risk of overfitting, a fraction of approximately 5% of the total dataset consisting of 2891 images was excluded. Figure 7 depicts the outcome of the proposed approach utilizing 11 epochs. Figure 8 depicts the training and validation accuracy as a function of the number of epochs, while Figure 9 displays the corresponding loss.

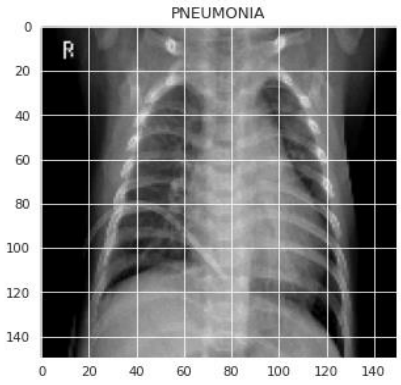

Fig. 6. Images with Pneumonia.

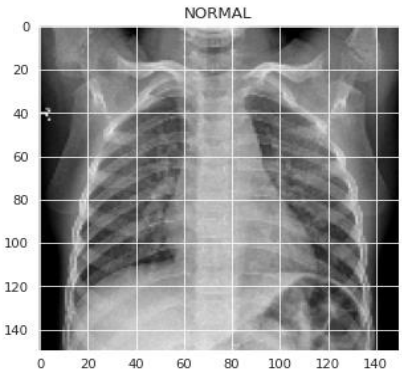

Fig. 7. Images with normal lung.

```
Epoch 1/12
163/163 [==============================] - 13s 83ms/step - loss: 0.5957 - accu
racy: 0.8357 - val_loss: 38.5047 - val_accuracy: 0.5000
Epoch 2/12
163/163 [==============================] - 12s 72ms/step - loss: 0.2812 - accu
racy: 0.8982 - val_loss: 30.2517 - val_accuracy: 0.5000
Epoch 3/12
163/163 [==============================] - 12s 72ms/step - loss: 0.2294 - accu
racy: 0.9135 - val_loss: 19.2671 - val_accuracy: 0.5625
Epoch 4/12
163/163 [==============================] - 11s 70ms/step - loss: 0.2118 - accu
racy: 0.9296 - val_loss: 28.6478 - val_accuracy: 0.5000
Epoch 5/12
163/163 [==============================] - 12s 74ms/step - loss: 0.1951 - accu
racy: 0.9310 - val_loss: 1.6000 - val_accuracy: 0.5000

Epoch 00005: ReduceLROnPlateau reducing learning rate to 0.0003000000142492354.
Epoch 6/12
163/163 [==============================] - 12s 72ms/step - loss: 0.1388 - accu
racy: 0.9513 - val_loss: 2.5989 - val_accuracy: 0.5625
Epoch 7/12
163/163 [==============================] - 12s 72ms/step - loss: 0.1344 - accu
racy: 0.9538 - val_loss: 23.3912 - val_accuracy: 0.5000

Epoch 00007: ReduceLROnPlateau reducing learning rate to 9.000000427477062e-05.
Epoch 8/12
163/163 [==============================] - 12s 71ms/step - loss: 0.1109 - accu
racy: 0.9641 - val_loss: 0.8426 - val_accuracy: 0.6875
Epoch 9/12
163/163 [==============================] - 12s 71ms/step - loss: 0.1078 - accu
racy: 0.9630 - val_loss: 1.3816 - val_accuracy: 0.5000
Epoch 10/12
163/163 [==============================] - 12s 77ms/step - loss: 0.1220 - accu
racy: 0.9622 - val_loss: 5.0193 - val_accuracy: 0.5000

Epoch 00010: ReduceLROnPlateau reducing learning rate to 2.700000040931627e-05.
Epoch 11/12
163/163 [==============================] - 12s 71ms/step - loss: 0.0965 - accu
racy: 0.9641 - val_loss: 3.0119 - val_accuracy: 0.5625
Epoch 12/12
```

Fig. 8. The completed product of our suggested procedure.

Table 2: Evaluation of the suggested ANN model's functionality.

NO. Image of Training	NO. Image Testing	Ratio of Splitting	Accuracy (%)
2169	493	8:2	98.14
2473	273	9:1	98.12

Table 3: Evaluation of Competencies.

Studies	Accuracy (%)
Seetha et al. [17]	97.50
Tonmoy Hossain et al. [18]	97.87
ANN Proposed system	98.14

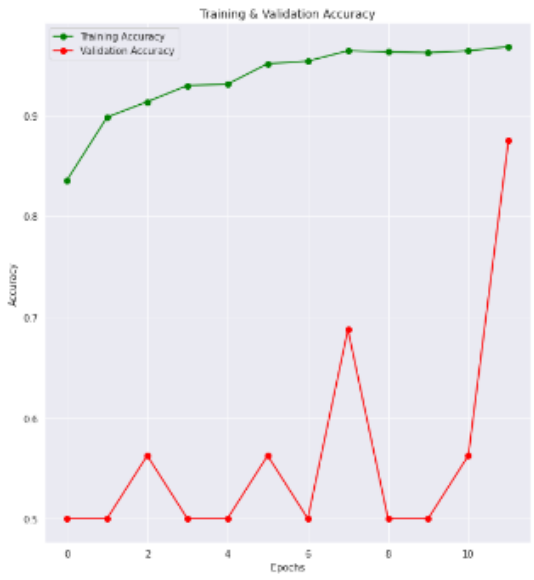

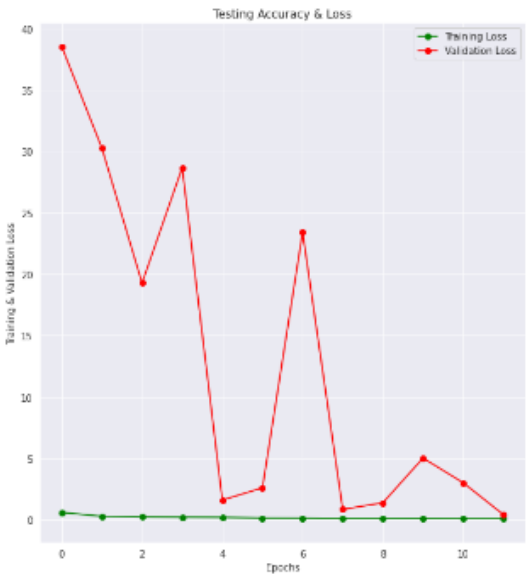

Fig. 9. Training and validation accuracy. **Fig. 10.** Training and validation loss.

As shown in Table 3, the accuracy of the proposed model is 98.14 percent, which is higher than the results found by Seetha et al. [17] and Tonmoy Hossain et al. [18]. Figure 10 depicts an example of the output image that can be anticipated.

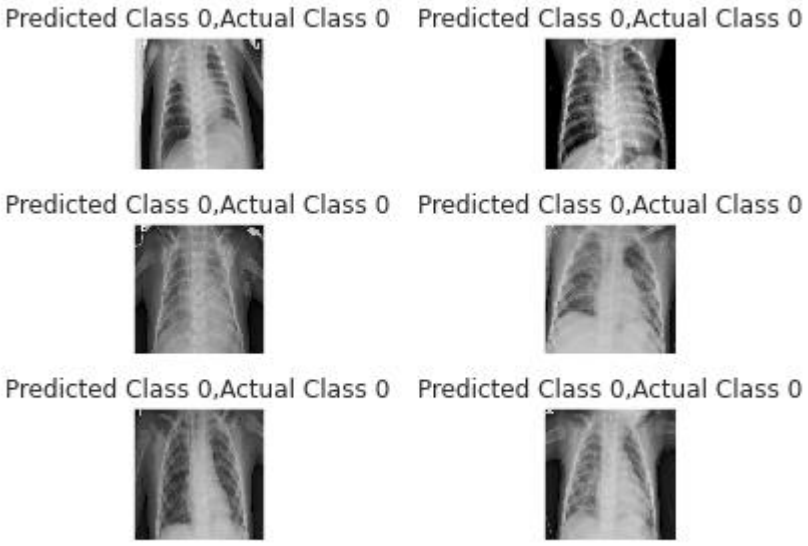

Fig. 11. Prediction by our proposed model.

6. Conclusion

Magnetic resonance imaging (MRI) is the gold standard when diagnosing and categorizing pneumonia. To improve the accuracy of multi-modal MRI images, convolutional neural networks (CNNs) can autonomously acquire complex features that differentiate between healthy brain tissues and pneumonia tissues. At first, an effort was made to use Support Vector Machine (SVM) with an ANN, but the resulting accuracy was only 23.53 percent. After that, we ran experiments with varying inputs to see what happened. The optimizer has been updated to AdaMax, and the final layer parameter has been modified to softmax. Subsequently, the precision rate was recorded at 94.10%.

Nevertheless, further experimentation was required, prompting us to modify the optimizer to RMSProp. As a result, the precision of the output was enhanced to 98.14%. The ultimate result was achieved by utilizing 4613 photographic data points for training and 252 images for testing, with a ratio of 9:1, employing an 11-epoch methodology. To mitigate overfitting, several photographs were also removed.

References

[1] E.C.f.D.P.a.C. (ECDC) Covid-19 situation update worldwide, as of 18 2020 (2020)

[2] Cascella M., Rajnik M., Cuomo A., Dulebohn S.C., Di Napoli R. Features, evaluation and treatment coronavirus (COVID-19) Statpearls [Internet], StatPearls Publishing (2020)

[3] ACR Recommendations for the use of chest radiography and computed tomography (CT) for suspected COVID-19 infection (2020)

[4] Wong H.Y.F., Lam H.Y.S., Fong A.H.-T., Leung S.T., Chin T.W.-Y., Lo C.S.Y., Lui M.M.-S., Lee J.C.Y., Chiu K.W.-H., Chung T. Frequency and distribution of chest radiographic findings in COVID-19 positive patients Radiology (2020), Article 201160

[5] Cho S., Lim S., Kim C., Wi S., Kwon T., Youn W.S., Lee S.H., Kang B.S., Cho S.

Enhancement of soft-tissue contrast in cone-beam CT using an anti-scatter grid with a sparse sampling approach Phys. Med., 70 (2020), pp. 1-9.

[6] Mijwil, Maad M., and Ehsan Ali Al-Zubaidi. "Medical image classification for coronavirus disease (COVID-19) using convolutional neural networks." Iraqi Journal of Science 62.8 (2021): 2740-2747.

[7] Alhelfi, Labiba M., and Hana M. Ali. "Using Persistence Barcode to Show the Impact of Data Complexity on the Neural Network Architecture." Iraqi Journal of Science (2022): 2262-2278.

[8] Shakeel P.M., Burhanuddin M., Desa M.I. Automatic lung cancer detection from CT image using improved deep neural network and ensemble classifier Neural Comput. Appl. (2020), pp. 1-14

[9] Hussein, Waleed Noori, and Haider N. Hussain. "A design of a hybrid algorithm for optical character recognition of online hand-written Arabic alphabets." Iraqi Journal of Science (2019): 2067-2079.

[10] Jacobi A., Chung M., Bernheim A., Eber C. Portable chest X-ray in coronavirus disease-19 (COVID-19): A pictorial review Clinic. Imag. (2020)

[11] Maleki N., Zeinali Y., Niaki S.T.A. A k-NN method for lung cancer prognosis with the use of a genetic algorithm for feature selection Expert Syst. Appl., 164 (2020), Article 113981

[12] Al-Tashi Q., Kadir S.J.A., Rais H.M., Mirjalili S., Alhussian H. Binary optimization using hybrid grey wolf optimization for feature selection IEEE Access, 7 (2019), pp. 39496-39508

[13] Masoumi A., Ghassem-zadeh S., Hosseini S.H., Ghavidel B.Z. Application of neural network and weighted improved PSO for uncertainty modeling and optimal allocating of renewable energies along with battery energy storage Appl. Soft Comput., 88 (2020), Article 105979

[14] Şenel F.A., Gökçe F., Yüksel A.S., Yiğit T. A novel hybrid PSO–GWO algorithm for optimization problems Eng. Comput., 35 (2019), pp. 1359-1373

[15]

Moosavi S.H.S., Bardsiri V.K. Satin bowerbird optimizer: A new optimization algorithm to optimize ANFIS for software development effort estimation Eng. Appl. Artif. Intell., 60 (2017), pp. 1-15

[16] Simon D. Biogeography-based optimization IEEE Trans. Evol. Comput., 12 (2008), pp. 702-713

[17] Karakonstantis I., Vlachos A. Bat algorithm applied to continuous constrained optimization problems J. Inform. Optim. Sci. (2020), pp. 1-19

[18] Mirjalili S., Mirjalili S.M., Hatamlou A. Multi-verse optimizer: a nature-inspired algorithm for global optimization Neural Comput. Appl., 27 (2016), pp. 495-513.